Communication

Photovoltaic Charge Generation Visualized at the Nanoscale: A Proof of Principle

Andrea Liscio, Giovanna De Luca, Fabian Nolde, Vincenzo Palermo, Klaus Mllen, and Paolo Samor

J. Am. Chem. Soc., **2008**, 130 (3), 780-781 • DOI: 10.1021/ja075291r

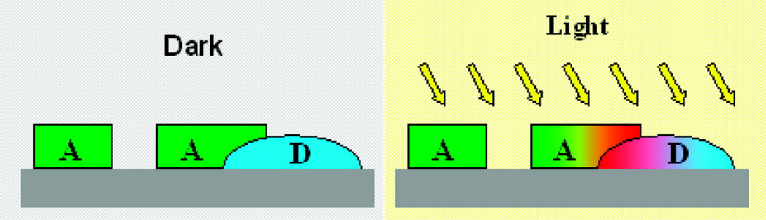

More About This Article

Additional resources and features associated with this article are available within the HTML version:

- Supporting Information
- Links to the 4 articles that cite this article, as of the time of this article download
- Access to high resolution figures
- Links to articles and content related to this article
- Copyright permission to reproduce figures and/or text from this article

View the Full Text HTML

J|A|C|S
COMMUNICATIONS

Published on Web 12/23/2007

Photovoltaic Charge Generation Visualized at the Nanoscale: A Proof of Principle

Andrea Liscio,[†] Giovanna De Luca,[†] Fabian Nolde,[‡] Vincenzo Palermo,*[,†] Klaus Müllen,*[,‡] and Paolo Samori*[,†,§]

ISOF−CNR, via Gobetti 101, 40129 Bologna, Italy, Max-Planck Institute for Polymer Research, Ackermannweg 10, 55124 Mainz, Germany, and ISIS−CNRS 7006, ULP, 8 allée Gaspard Monge, 67000 Strasbourg, France

Received July 16, 2007; E-mail: palermo@isof.cnr.it; muellen@mpip-mainz.mpg.de; samori@isis-ulp.org

Among molecular electronic devices, plastic solar cells[1] are gathering a great interest as a potential alternative energy source in a world of increasing demand for energy and declining reserve of the conventional energy resources.[2] Organic solar cells have the advantage of being cheap and easily processable, albeit their power conversions, reaching nowadays up to 5%,[3] remains low compared to their Si counterparts. Organic solar cells consist of a blend of electron acceptor (A) and donor (D) assemblies phase-segregated on the tens of nanometer scale, that is, a scale comparable to the mean exciton diffusion length. The excitons photogenerated in the device are split into free electrons and holes by the difference in HOMO−LUMO levels of the two materials.[4] These layers' thickness typically ranges from tens to hundreds of nanometers, and the two materials are always in close physical contact, forming a complex interface. To improve the solar cells' performance, it is of key importance to unravel in real-time the generation and transfer of charges between A and D phases on the nanoscale on structurally defined architectures. This goal is often difficult to accomplish with conventional 3D solar cell prototypes.

Here we study the charge photogeneration in quasi-2D systems, that is, ultrathin layers of phase-segregated A−D blends, with a particular focus on understanding the contribution of the physical contact between A:D phases to the charge transfer in photovoltaic films. Under such conditions, with the lateral size of the films being several hundreds of nanometers, that is, much larger than their thickness, the charges are virtually vertically confined in a few nanometers, but they can move parallel to the substrate plane over much larger distances.

Morphological and electronic properties of thin films can be studied with a nanoscale resolution by atomic force microscopy (AFM)[5] and Kelvin probe force microscopy (KPFM),[6] respectively. In particular, KPFM allows quantitative mapping of the electronic properties of nanostructures, that is, determination of the surface potential (SP) of nano-objects with a lateral and potential resolution below 70 nm and 10 mV, respectively.[6] It thus enables real-time explorations of the photovoltaic effect, as proven on photovoltaic films with thicknesses of 50−200 nm.[7,8] By highlighting the presence of charge percolation paths, defects, and bottlenecks within the film, it can provide useful insight for the improvement of the performance of solar cells.

We chose a blend of regioregular poly(3-hexylthiophene) (P3HT)[9] (Figure 1a) and *N*,*N*′-bis(1-ethylpropyl)-3,4:9,10-perylenebis(dicarboximide) (PDI)[10] (Figure 1b) as model systems, acting as D and A, respectively. Although blends of these materials are known not to exhibit the best photovoltaic performance, they are able to self-assemble into structurally defined and ordered architectures. The two molecules are cast from $CHCl_3$ solutions on a Si substrate covered by a few nanometer thick layer of native oxide (SiO_x; experimental details are given in the Supporting Information).

[†] ISOF−CNR.
[‡] Max-Planck Institute for Polymer Research.
[§] ISIS−CNRS.

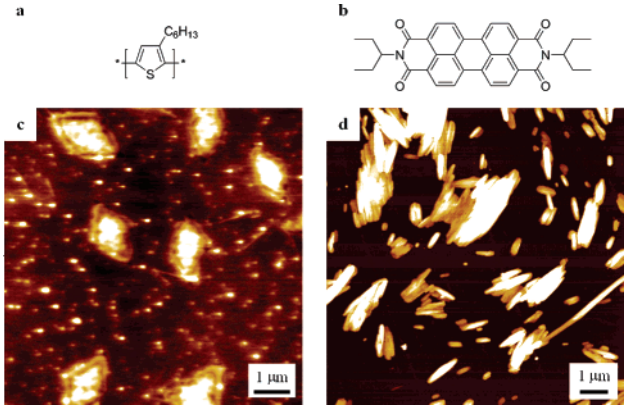

Figure 1. Chemical structures of (a) poly(3-hexylthiophene) (P3HT) and (b) *N*,*N*′-bis(1-ethylpropyl)-3,4:9,10-perylenebis(dicarboximide) (PDI). (c,d) Topographical AFM images of (c) P3HT and (d) PDI films adsorbed on SiO_x. *Z*-scales: (c) 10 nm and (d) 60 nm.

AFM images of neat films of P3HT on SiO_x reveal that most of the material aggregates into rhomboidal structures, although short ribbons and smaller spherical clusters are also observed at the surface (Figure 1c). These rhomboidal aggregates are ca. 1 μm wide and 13 ± 2 nm thick, whereas the surrounding ribbons have a width of 120 ± 10 nm and a height of 8 ± 2 nm. Conversely, PDI films on SiO_x exhibit a more complex morphology consisting of needle-like assemblies (Figure 1d) having a width of 300 ± 50 nm, a height of 30 ± 3 nm, and a broad range of lengths spanning from a few hundred nanometers to some micrometers.[11] KPFM revealed that the molecular aggregates of the two species show different SPs with respect to that of the substrate (see Figure SI1 in Supporting Information).

Films of PDI and P3HT were co-deposited by drop casting at surfaces in a two-step deposition. They exhibit coexistence of P3HT rhomboidal aggregates, having more irregular shapes, and PDI small clusters, featuring lateral dimensions >50 nm and thickness ∼30 nm. The overall film morphology appears more disordered (Figure 2b). Some of these clusters (indicated with I) are adsorbed as isolated nano-objects on the neat substrate surface, whereas others (II) are on top of the P3HT architectures (III).

A cartoon describing such a peculiar morphology is displayed in Figure 2a, whereas Figure 2c shows the KPFM image recorded under dark conditions, and the relative measured SP values, averaged over all the collected measurements, are summarized in Table 1. For the sake of simplicity, the substrate is used as reference and its SP value leveled to zero. The measured SP of P3HT structures is about −30 mV, while that of PDI clusters of type I is not much larger than the noise level (∼10 mV). Both values are in agreement with those measured on neat films (see Supporting Information). Differently, the PDI clusters in physical contact with the P3HT aggregates (type II) show an SP value of −40 mV, being closer than that of P3HT. The difference in SP for the two types of

10.1021/ja075291r CCC: $40.75

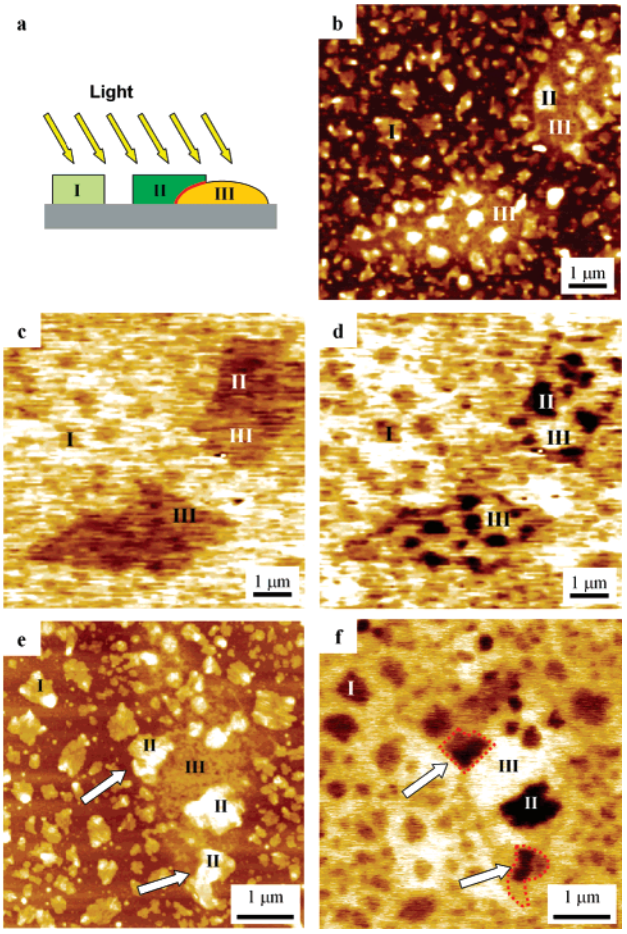

Figure 2. (a) Carton of illuminated sample showing both P3HT:PDI (**III: II**, respectively) aggregates and isolated PDI assemblies (**I**). (b) Topographical image of P3HT:PDI agglomerates, and corresponding KPFM images recorded (c) in dark and (d) under illumination. (e,f) Topographical and KPFM images recorded under illumination on a different zone of the sample, showing PDI clusters partially in contact with P3HT (white arrows), which boundaries are marked in (f) by a dot contour. *Z*-scales: (b) 20 nm, (c,d) 60 mV, (e) 37 nm, and (f) 90 mV.

Table 1. SPs of P3HT and PDI Measured for Sample under Dark and Light Irradiation[a]

	SP (mV)		
	P3HT (type III)	PDI (type II)	PDI (type I)
dark	-30 ± 5	-40 ± 5	-12 ± 4
light	-10 ± 5	-90 ± 10	-32 ± 5
dark − light	-20 ± 7	50 ± 11	20 ± 7

[a] SPs are given as differences with respect to substrate SP. The error bars are the variances obtained by averaging over all the collected measurements.

PDI clusters can be ascribed (1) to a possible different shift of the energy levels (or band bending) at the PDI:SiO_x and PDI:P3HT interfaces, as shown by Kampen[12] for perylene derivatives, and (2) to a non-negligible contribution of the underlying material's SP to the measured signal.

Upon illumination with white light (Figure 2d), the SP of the P3HT phase (III) becomes more positive and displays a value close to that of the substrate, while the SP of both PDI clusters, that is, the isolated ones (I) and those in contact with P3HT (II), becomes more negative at −30 and −90 mV, respectively. A negative shift of the average SP is also observed, due to the effect of charges drifting into the substrate.[8] To avoid underestimation of the SP values on smaller clusters due to the averaging of the SP signal sampled at a given position, our statistical analyses were performed only on clusters with a lateral size over 150 nm (see Supporting Information), thus larger than the effective area of the SP measurement.[13] Figure 2e shows a more detailed image of the blend morphology, where some PDI structures of type II exhibit only a portion of the cluster in physical contact with P3HT (white arrows). In the KPFM image (Figure 2f), the boundaries of these PDI clusters are marked with a dot contour. The portion in contact with the P3HT film shows a different SP when compared to the part directly adsorbed on the neat substrate. The number of charges needed to vary significantly the potential of such a nanometer cluster is very small and can be quantified by KPFM. Taking into account the effective area, we can estimate the charge generated on illumination for all the PDI clusters. In a first rough approximation, the PDI clusters can be considered as charged discs: under this assumption, the number of charges, Δq, generated upon illumination is directly proportional to the potential shift: $\Delta V = \Delta q/(\pi \epsilon d)$, where d and ϵ are the diameter and the permittivity of the cluster, respectively. This reveals that only very few electrons (below 10) are generated in each PDI cluster, although this number depends greatly on the size and shape of the cluster.

In summary, the KPFM images of P3HT:PDI blends provide a nanoscale resolved proof of principle of the photovoltaic activity in a phase-segregated electron acceptor−donor blend architecture. The same type of molecular assemblies, obtained from a given electron-accepting material on the same sample, shows different SP changes upon white-light illumination when in physical contact with the donor materials or isolated from it. Although excitons are generated by light absorption in all the PDI clusters, we unambiguously proved that only the ones which are in contact with P3HT exhibit an appreciable charge transfer because of the existence of a complementary electron donor phase.

Acknowledgment. This work was supported by the Projects ESF-SONS2-SUPRAMATES, Regione Emilia-Romagna PRIITT Nanofaber Net-Lab, EU-ForceTool (NMP4-CT-2004-013684), and EU-Marie Curie EST-SUPER (MEST-CT-2004-008128).

Supporting Information Available: Experimental details and KPFM images of P3HT and PDI aggregates on SiO_x (Figure SI1). This material is available free of charge via the Internet at http://pubs.acs.org.

References

(1) (a) Halls, J. J. M.; Walsh, C. A.; Greenham, N. C.; Marseglia, E. A.; Friend, R. H.; Moratti, S. C.; Holmes, A. B. *Nature* **1995**, *376*, 498. (b) Yu, G.; Gao, J.; Hummelen, J. C.; Wudl, F.; Heeger, A. J. *Science* **1995**, *270*, 1789.
(2) Armaroli, N.; Balzani, V. *Angew. Chem., Int. Ed.* **2007**, *46*, 52.
(3) (a) Li, G.; Shrotriya, V.; Huang, J.; Yao, Y.; Moriarty, T.; Emery, K.; Yang, Y. *Nat. Mater.* **2005**, *4*, 864. (b) Ma, W.; Yang, C.; Gong, X.; Lee, K.; Heeger, A. J. *Adv. Funct. Mater.* **2005**, *15*, 1617. (c) Reyes-Reyes, M.; Kim, K.; Carroll, D. L. *Appl. Phys. Lett.* **2005**, *87*, 083506.
(4) Hoppe, H.; Sariciftci, N. S. *J. Mater. Res.* **2004**, *19*, 1924.
(5) Samorì, P. *Chem. Soc. Rev.* **2005**, *34*, 551.
(6) Palermo, V.; Palma, M.; Samorì, P. *Adv. Mater.* **2006**, *18*, 145.
(7) (a) Hoppe, H.; Glatzel, T.; Niggemann, M.; Hinsch, A.; Lux-Steiner, M. C.; Sariciftci, N. S. *Nano Lett.* **2005**, *5*, 269. (b) Palermo, V.; Ridolfi, G.; Talarico, A. M.; Favaretto, L.; Barbarella, G.; Camaioni, N.; Samorì, P. *Adv. Funct. Mater.* **2007**, *17*, 472. (c) Coffey, D. C.; Ginger, D. S. *Nat. Mater.* **2006**, *5*, 735.
(8) Chiesa, M.; Burgi, L.; Kim, J.-S.; Shikler, R.; Friend, R. H.; Sirringhaus, H. *Nano Lett.* **2005**, *5*, 559.
(9) Sirringhaus, H.; Brown, P. J.; Friend, R. H.; Nielsen, M. M.; Bechgaard, K.; Langeveld-Voss, B. M. W.; Spiering, A. J. H.; Janssen, R. A. J.; Meijer, E. W.; Herwig, P.; de Leeuw, D. M. *Nature* **1999**, *401*, 685.
(10) (a) Elemans, J. A. A. W.; Van Hameren, R.; Nolte, R. J. M.; Rowan, A. E. *Adv. Mater.* **2006**, *18*, 1251. (b) Würthner, F. *Chem. Commun.* **2004**, 1564.
(11) Palermo, V.; Liscio, A.; Gentilini, D.; Nolde, F.; Müllen, K.; Samorì, P. *Small* **2007**, *3*, 161.
(12) Kampen, T. U.; Das, A.; Park, S.; Hoyer, W.; Zahn, D. R. T. *Appl. Surf. Sci.* **2004**, *234*, 333.
(13) Liscio, A.; Palermo, V.; Gentilini, D.; Nolde, F.; Müllen, K.; Samorì, P. *Adv. Funct. Mater.* **2006**, *16*, 1407.

JA075291R